Interfacial Effects in Polypropylene–Silica Nanocomposites

Min Zhi Rong,[1] Ming Qiu Zhang,[1] Shun Long Pan,[1] Klaus Friedrich[2]

[1]*Key Laboratory for Polymeric Composite and Functional Materials of the Ministry of Education, Materials Science Institute, Zhongshan University, Guangzhou 510275, People's Republic of China*
[2]*Institute for Composite Materials, University of Kaiserslautern, D-67663 Kaiserslautern, Germany*

Received 27 January 2003; accepted 8 December 2003

ABSTRACT: Grafted inorganic nanoparticles can greatly improve the mechanical performance of polymers. To examine the effects of the interfacial characteristics generated by the grafting polymer bonded to nanoparticle surfaces, we chemically grafted nano-silica with different polymers and then melt-mixed it with polypropylene (PP). We extracted the homopolymers produced during the graft polymerization from the grafted products before the composites were manufactured to get rid of the side effects of the nongrafting polymers. We tailored the interfacial interaction between the grafted nano-SiO_2 and PP matrix by changing the amount of the grafting polymers on the nanoparticles, that is, the grafting percentage. Mechanical tests indicated that all the composites incorporated with grafted nano-SiO_2 particles possessed much higher impact strength than untreated SiO_2/PP composites and neat PP. The greatest contribution of the particles was made at a low grafting percentage. Tensile measurements showed that the treated nanoparticles could provide PP with stiffening, strengthening, and toughening effects at a rather low filler content (typically 0.8 vol %) because of the enhanced interfacial adhesion resulting from molecular entanglement and interdiffusion between the grating polymers on the nanoparticles and matrix macromolecules. The presence of grafting polymers on the nanoparticles provided the composites with a tailorable interphase. The tensile performance of the composites was sensitive to the nature of the grafting polymers. Basically, a hard interface was beneficial to stress transfer, whereas a soft one hindered the development of cavities in the matrix.
 J Appl Polym Sci 92: 1771–1781, 2004

Key words: interfaces; mechanical properties; nanocomposites; silicas; structure-property relations

INTRODUCTION

Polymer nanocomposites comprise a new class of materials in which nanoscale particulates (e.g., clay or other inorganic minerals) are finely dispersed within the matrices. In comparison with neat polymers and microparticulate composites, these materials have been reported to exhibit markedly improved properties, including modulus, strength, barrier performance, solvent and heat resistance, and optical transparency.[1–3] Furthermore, these improvements are achieved at low concentrations of the inorganic components (1–10 wt %); this contrasts strongly with conventional filled polymers, which generally require high loadings within the range of 25–40 wt %. In this context, the nanocomposites are much lighter in weight and are more easily processed.

However, polymer-based nanocomposites are very difficult to make with the processing techniques common to conventional plastics because of the strong tendency of nanoparticles to agglomerate, which is hardly to be overcome by the limited shear force during compounding. To break down nanoparticle agglomerates and to produce nanostructured composites, researchers have attempted many specific routes in recent years, such as the sol–gel method,[4] *in situ* intercalative polymerization,[5,6] and *in situ* polymerization in the presence of nanoparticles.[7] With respect to the cost effectiveness and feasibility of the available processing techniques, melt-blending nanoparticles with polymers is still the optimum method of compounding for the mass production of nanocomposites based on polyolefins. With the help of particulate modification or mixing technique improvement, for example, some works on polypropylene (PP) nanocomposites containing nonlayered nanoparticles and anisotropic nanoparticles derived from organophilic layered silicates have already demonstrated effective matrix reinforcement at low filler fractions. Comparatively, PP/clay nanocomposites have been extensively studied.[8–10] These composite materials exhibit good

Correspondence to: M. Z. Rong (cesrmz@zsu.edu.cn).
Contract grant sponsor: Deutsche Forschungsgemeinschaft; contract grant number: DFG FR675/40-1.
Contract grant sponsor: National Natural Science Foundation of China; contract grant numbers: 50133020 and 50273047.
Contract grant sponsor: Team Project of the Natural Science Foundation of Guangdong, China; contract grant number: 20003038.
Contract grant sponsor: Key Program of the Science and Technology Department of Guangdong, China; contract grant number: A1070201.

Journal of Applied Polymer Science, Vol. 92, 1771–1781 (2004)

general properties when the layered silicates can be exfoliated, but the tailoring ability of the interface is limited.

However, very few works have been devoted to research on PP filled with nonlayered inorganic nanoparticles. Chan et al.[11] reported that an increase in the Izod impact strength by a factor of approximately 300% was obtained when nanosize calcium carbonate was incorporated into PP via melt mixing with a Haake mixer. Wang et al.[12] showed that the mechanical properties of PP, especially the ductile properties, were effectively improved by the incorporation of stearic acid modified nano-$CaCO_3$ in an ultra-high-speed mixer. In this way, modified nano-$CaCO_3$ can disperse uniformly in the matrix even at a high content (more than 15 vol %). Saujanya and Radhakrishnan[13] studied the isothermal crystallization behavior of a PP/nano-calcium phosphate system and found that the crystallization rate drastically increased; this resulted in a rapid decrease in the ultimate spherulite sizes.

In our previous works, an irradiation grafting polymerization method was used to modify the nonlayered nanoparticles such as silica and calcium carbonate first, and then the treated particles were mechanically mixed with PP as usual.[14] The mechanical testing of PP filled with nano-SiO_2[15–17] and nano-$CaCO_3$[14,18] demonstrated the feasibility of this approach. Only a small amount of the treated nanoparticles (typically less than 3 vol %) can simultaneously improve the stiffness, strength, toughness, and thermal deformation temperature of the matrix. As an explanation for the specific influence generated by the nanoparticles at a low-filler-content regime, a double percolation of stress volumes, characterized by the appearance of connected shear yielded networks throughout the composite, was proposed.[19] The distinct advantage of this pretreatment is that the interfacial tailoring becomes quite easy through the adjustment of the species of the grafting monomers and through changes in the grafting yielding. As a result, one may obtain the preferred structure of each component comprising the final composites.

In fact, the outstanding characteristics of polymer nanocomposites originate mainly from their ultrafine phase dimensions. The properties of the composites are strongly dependent on the nature of the filler–matrix interface. The control and manipulation of the surface properties of the nanoparticles are, therefore, very important. To develop an understanding of the important role of interfacial interactions in the properties of PP composites filled with modified nanosilica, we added different grafting polymers to the surfaces of silica nanoparticles through a chemical grafting reaction in a solvent. In addition, the homopolymers surrounding the nanoparticles produced during the grafting polymerization were removed before the melt compounding so that the complexity of the composites was reduced. Although the particle treatments (i.e., chemical grafting and homopolymer isolation) are not practical enough from an engineering perspective in comparison with the technical route applied in our earlier experiments (i.e., irradiation grafting and homopolymer retention over the course of melt blending),[14–19] it is necessary to carry out this investigation because the current system can be taken as a model material. The outcomes will be provided with more explicit scientific meaning accordingly.

EXPERIMENTAL

Materials

An isotactic PP homopolymer (F401) was supplied by Guangzhou Petroleum Chemical Co. (Guangzhou, China). It had a melt-flow index of 18.3 g/10 min (2.16 kg at 230°C). Nano-SiO_2 with an average primary particle size of 10 nm and a specific surface area of 640 m^2/g was purchased from Zhoushan Nanomaterials Co. (Zhoushan, China). Various commercial monomers (styrene, methyl methacrylate, ethyl acrylate, and butyl acrylate) were used as grafting monomers without further purification.

Chemical grafting of nano-SiO_2

The introduction of double bonds (i.e., reactive groups) onto the surfaces of SiO_2 nanoparticles was achieved by the reaction of silane KH570 (γ-methacryloxypropyl trimethoxy silane) with the hydroxyl groups of SiO_2. A mixture of equal amounts of silica nanoparticles and KH570 in 300 mL of a 95% alcohol solution was refluxed at the boiling temperature of the solution for 4 h with stirring. Afterward, the particles were collected by filtration, dried *in vacuo* (at 80°C for 24 h), and extracted with alcohol for 24 h to remove the excessively absorbed silane. Then, the KH570-treated SiO_2 was air-dried and allowed to react at 80°C *in vacuo* for 24 h. The content of the silane attached to the SiO_2 surfaces by the aforementioned treatment was 2.2 wt %, as detected by a Shimadzu TA-50 thermogravimeter (Kyoto, Japan).

To obtain grafted nano-SiO_2 with the aforesaid monomers, we mixed the KH570-pretreated particles with toluene under sonication for 30 min. Then, the initiator, azobisisobutyronitrile (AIBN), was added with stirring to the reactor, which had been kept at certain temperature and protected with N_2. The monomers were incorporated into the system 5 min later. The reaction went on for several hours, and then the product was obtained from the filtration of the resultant suspension.

Characterization of the grafted products

To evaluate the results of grafting and to characterize the grafted nanoparticles, we separated the grafting polymer and the homopolymer that were generated during the grafting polymerization of the monomers. For this purpose, the dried product (weight W_1) was extracted with a suitable solvent [toluene for polystyrene (PS) and acetone for poly(methyl methacrylate) (PMMA), poly(ethyl acrylate) (PEA), and poly(butyl acrylate) (PBA)] in a Soxhlet apparatus for 72 h to isolate the polymer-grafted SiO_2 (weight W_2) from the absorbed homopolymers. Then, the dried grafted nanoparticles with different grafting polymers (denoted SiO_2-*g*-PS, SiO_2-*g*-PMMA, SiO_2-*g*-PEA, and SiO_2-*g*-PBA, respectively) were transferred to a Shimadzu TA-50 thermogravimeter to determine the grafting percentage (γ_g). Here, the weight fraction of KH570 was deducted from the values of γ_g. The nongrafted polymer in the supernatant solution was precipitated through the addition of the solution to methanol. The resultant precipitate was filtered, washed, and dried *in vacuo* at 80°C so that we could estimate the amount of the homopolymer (weight W_3). The monomer conversion (γ_c) and grafting efficiency (γ_e) were calculated as follows:

$$\gamma_c = [(W_1 - W_2) + \gamma_g W_o - W_{AIBN}]/W_m$$

$$\gamma_e = \gamma_g W_o / \gamma_c W_m$$

where W_{AIBN} is the weight of the initiator AIBN and W_m and W_o denote the weights of the monomer and SiO_2, respectively.

A Nicolet 210 Fourier transform infrared (FTIR) spectroscope (Pittsfield, MA) was used to characterize the chemical structures of the modified nanoparticles. X-ray photoelectron spectroscopy (XPS) images of the grafted nanoparticles were collected with a LAB ZZOI-XL apparatus (Thermo Electron Corp., Houston, TX) to illuminate the interaction between the particles and the grafted polymer chains. The molecular weights of the grafted and homopolymerized polymers were determined with a Waters 410 gel permeation chromatograph (Milford, MA), with tetrahydrofuran as the solvent. The grafting polymer was obtained by the removal of silica from the grafted particles with a 20% HF solution. For the observation of the morphologies of the nanoparticles, untreated SiO_2 and treated SiO_2 were added to ethanol and toluene to prepare 0.001 g/mL solutions, respectively. With the aid of sonication for 60 min, the solutions were transferred to glass slides. After the evaporation of the solvents, a Hitachi S-520 scanning electron microscope (Tokyo, Japan) was used to examine the appearance of the particles.

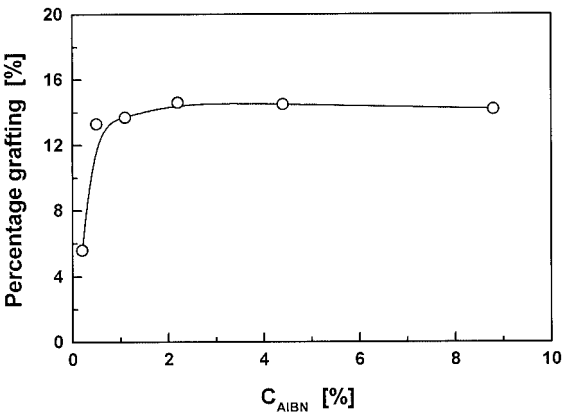

Figure 1 Effect of the initiator concentration (C_{AIBN}; expressed in terms of the molar ratio of AIBN to silica) on γ_g of styrene grafted onto nano-SiO_2 [C_{SiO_2} (molar concentration of nano-SiO_2 particles in the solvent) = 0.67 mol/L, C_{KH570} (molar concentration of KH570 attached to the nano-SiO_2 surface in the solvent) = 3.56 mmol/L, C_{St} (molar ratio of styrene over silica) = 173%, reaction temperature = 80°C, reaction time = 8 h].

Composite preparation and characterization

Before being compounded with the PP matrix, all the grafted nano-silica particles were extracted with solvent for the removal of the homopolymer. The nanoparticles were first mixed with PP powder (1:2 w/w) with a ball mill. Then, the mixture was melt-mixed and diluted to the desired filler loading in a laboratory-size Brabender XB20-80 plasticorder (Duisberg, Germany) under standard experimental conditions (200°C, 60 rpm, and 8 min). After being removed and granulated, the blends were compression-molded into sheet samples (65 mm × 45 mm × 3 mm). Specimens of desired size for mechanical tests were machined from the compressing-molding plaques according to ref. 15. An XJJ-5 tester (Testing Machine Corp., Chengde, China) was used for measuring the unnotched Charpy impact strength. Room-temperature tensile testing of the composites was conducted on a Hounsfield 5KN universal testing machine (Surrey, UK) at a crosshead speed of 10 mm/min. Five samples were tested for each case. The fractured surfaces of the samples were also observed with a Hitachi S-520 scanning electron microscope at an accelerating voltage of 20 kV.

RESULTS AND DISCUSSION

Influence of the reaction conditions and chemical structure of grafted nano-SiO_2

Because our aim is to study the tailoring of the interface in PP composites by the modified nano-silica, we will discuss the effects of the reaction conditions on the grafting of the particles. Figure 1 shows the typical dependence of γ_g on the initiator concentration for

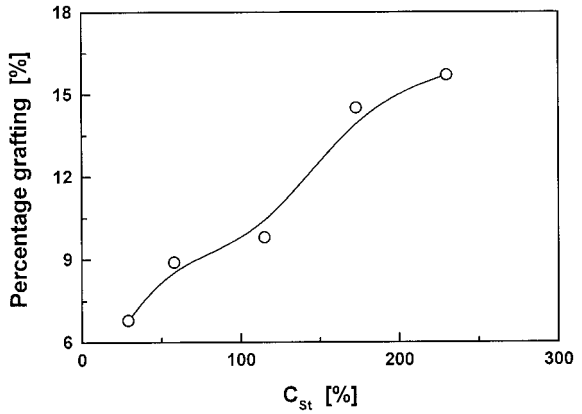

Figure 2 Effect of C_{St} on γ_g of styrene grafted onto nano-SiO_2 (C_{SiO_2} = 0.67 mol/L, C_{KH570} = 3.56 mmol/L, C_{AIBN} = 2.2%, reaction temperature = 80°C, reaction time = 8 h; see Fig. 1 for the definitions of the terms).

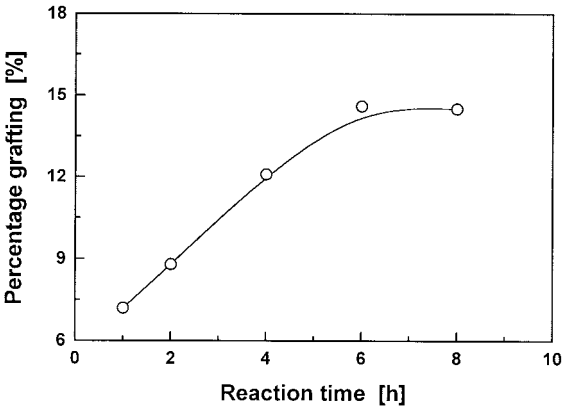

Figure 3 Effect of the reaction time on γ_g of styrene grafted onto nano-SiO_2 (C_{SiO_2} = 0.67 mol/L, C_{KH570} = 3.56 mmol/L, C_{AIBN} = 2.2%, C_{St} = 173%, reaction temperature = 80°C; see Fig. 1 for the definitions of the terms).

styrene grafting. γ_g sharply increases at rather low initiator (AIBN) concentrations and then declines slightly when the concentration is greater than 2.2%. This drastic increase is understandable because a higher initiator concentration would lead to a higher initiation rate, and so more double bonds on the surface can be initiated. The decreasing trend of γ_g implies that the termination of the initiator takes effect. Therefore, a suitable initiator concentration of 2.2% was chosen for the subsequent chemical grafting modification of nano-SiO_2.

For a similar system, the effects of the monomer concentration on the grafting reaction are shown in Figure 2 and Table I. The higher the monomer concentration is, the higher γ_g is. This phenomenon can be attributed to the fact that the polymerization rate increases with the monomer concentration. As a result, there is a greater probability of the monomers reacting with the double bonds on the nanoparticle surfaces at the beginning of the reaction. It is thus concluded that the amount of the grafting polymers chemically attached to nano-SiO_2 can be controlled through changes in the monomer concentration during the grafting polymerization. Because interfacial interactions in grafted nanoparticle/polymer composites deal with molecular entanglement and interdiffusion between the molecules of the grafting polymer on the nanoparticles and the matrix,[16] when the grafted nanoparticles are incorporated into the PP matrix, different degrees of interfacial interaction might be expected for different monomer concentrations and different species of the grafting monomers as well.

TABLE I
Influence of γ_c on γ_g onto Nano-SiO_2

Material	$C_{monomer}$ (%)[a]	γ_g (%)	γ_c (%)	γ_e (%)
SiO_2-*g*-PS	29	5.6	31	36
	58	10.2	31	35
	115	14.8	24	31
	230	16.2	21	19
SiO_2-*g*-PMMA	12	2.8	58	24
	30	14.1	54	52
	60	17.9	53	34
	120	20.8	47	22
SiO_2-*g*-PEA	12	4.4	65	34
	30	18.2	62	59
	60	21.3	55	39
	120	24.0	45	26
SiO_2-*g*-PBA	9	6.5	67	49
	23	11.9	56	42
	47	14.7	52	28
	94	20.9	51	21

Reaction conditions: C_{SiO_2} = 0.67 mol/L, C_{KH570} = 3.56 mmol/L, C_{AIBN} = 2.2%, reaction temperature = 80°C, and reaction time = 8 h (see Fig. 1 for the definitions of the terms).

[a] $C_{monomer}$ = molar ratio of the monomer to silica.

However, the data in Table I indicate that both γ_c and γ_e tend to decrease at higher monomer concentrations. This suggests that the growth of the grafting polymer is more significant for low monomer concentrations, and homopolymerization hinders the growth of the grafting polymer under high monomer concentrations.

In general, γ_g should increase with the reaction time. Figure 3 demonstrates that γ_g can be more than doubled with a rise in the reaction time from 1 to 6 h, and then it remains unchanged. Although toluene is a good solvent for both styrene and PS, the dependence of γ_g on the reaction time illustrated in Figure 3 reflects that the blocking effect of the grafting polymer chains on the diffusion of the monomers still exists. In fact, even when the reaction time is set at 8 h, γ_c is less than 70%, regardless of the monomer species and concentration (Table I); this means that the grafting reaction takes place mainly at the beginning of the reaction.

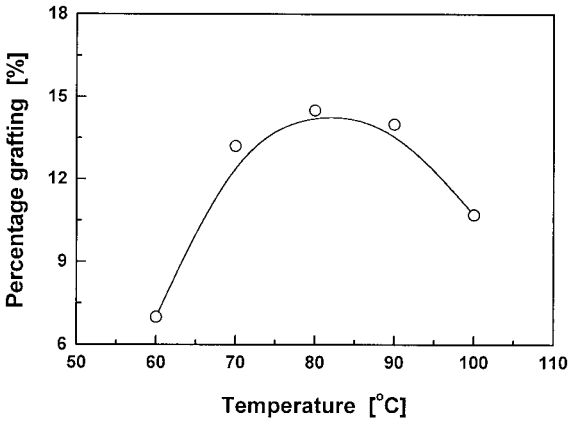

Figure 4 Effect of the reaction temperature on γ_g of styrene grafted onto nano-SiO_2 (C_{SiO_2} = 0.67 mol/L, C_{KH570} = 3.56 mmol/L, C_{AIBN} = 2.2%, C_{St} = 173%, reaction time = 8 h; see Fig. 1 for the definitions of the terms).

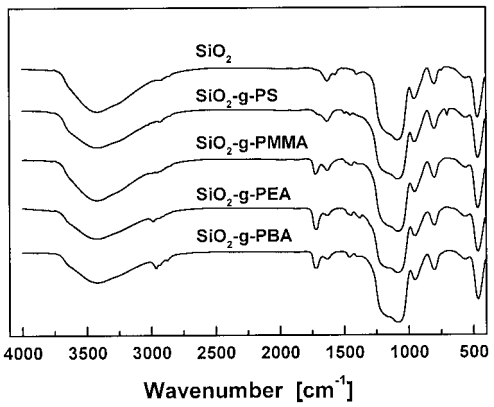

Figure 5 FTIR spectra of untreated and grafted nano-SiO_2 (γ_g = 14.8% for SiO_2-*g*-PS, 14.1% for SiO_2-*g*-PMMA, 18.2% for SiO_2-*g*-PEA, and 14.7% for SiO_2-*g*-PBA). To get rid of the influence of the homopolymers, we had to remove the nongrafted polymers from the grafted nanoparticles by extraction before the FTIR examination.

The dependence of γ_g on the reaction temperature also reveals that the grafting polymeric chains block the diffusion of the monomers. With increasing reaction temperature, as shown in Figure 4, γ_g shows an increasing trend due to the rise in the polymerization rate. However, a further increase in the reaction temperature results in a polymerization that is too fast: the grafting chains obstruct the monomers from diffusing toward the particle surface. Consequently, the grafting density has to be reduced because of the lack of monomer in contact with the surface of the nanoparticles. In this work, a reaction temperature of 80°C was fixed for producing the modified nano-SiO_2 used in the PP composites.

The number-average and weight-average molecular weights of both grafting and homopolymerized PS in SiO_2-*g*-PS are shown in Table II as functions of γ_g. Clearly, the grafting polymers collected from grafted nano-SiO_2 at different values of γ_g have similar molecular weights. That is, the aforementioned increase in the amount of the grafting polymer with an increasing monomer concentration originates predominately from the increase in the grafting density per surface area of the nanoparticles and not from the increase in the molecular length of the grafting polymer.

TABLE II
M_n and M_w Values for Grafting PS and Homopolymerized PS in SiO_2-*g*-PS

γ_g (%)	Material	M_n ($\times 10^4$)	M_w ($\times 10^4$)	M_w/M_n
4.64	Grafting PS	0.75	1.10	1.70
	Homopolymerized PS	0.76	1.30	1.46
14.8	Grafting PS	0.65	1.03	1.57
	Homopolymerized PS	0.94	1.37	1.59

M_n = number-average molecular weight; M_w = weight-average molecular weight.

That the molecular weight of the homopolymer is higher than that of the grafting polymer can be ascribed to the higher mobility of the nanoparticles in comparison with conventional microparticles, which makes chain termination between radicals easier. Besides, both grafting PS and homopolymer PS exhibit quite narrow molecular weight distributions. This means that the effect of the grafting polymer on the interfacial interaction in the subsequent PP composites can focus on γ_g rather than on the molecular distribution.

FTIR spectra of untreated and grafted nano-silica are shown in Figure 5. In comparison with the spectrum of SiO_2 as received, the adsorptions at 700 and 1400–1600 cm^{-1} appearing in the spectrum of SiO_2-*g*-PS represent the bending mode of C—H in benzene rings. Additionally, the bands around 1700 cm^{-1} in the spectra of SiO_2-*g*-PMMA, SiO_2-*g*-PEA, and SiO_2-*g*-PBA indicate the existence of carbonyl groups. These prove that PS, PMMA, PEA, and PBA are chemically connected to the surface of the nano-silica, and the grafting polymer chains cannot be removed by the extraction procedure. Figure 6 shows the difference between grafting PS and homopolymerized PS. The appearance of wide bands corresponding to a hydrogen bond (3100–3700 cm^{-1}) for grafting PS, which cannot be perceived for the PS homopolymer, reveals the existence of Si—O—C bonds between grafting PS and KH570-treated silica. Also, the stretching peaks of the carbonyl group at 1700 cm^{-1} and Si—O—Si at 1000–1150 cm^{-1} are indicative of KH570 in grafting PS, which reacts with styrene by the double bonds.

The strong interaction between nano-silica and grafting PS can be roughly evaluated from the thermal stability of SiO_2-*g*-PS, which is considerably higher than that of grafting PS. As shown in Figure 7, the

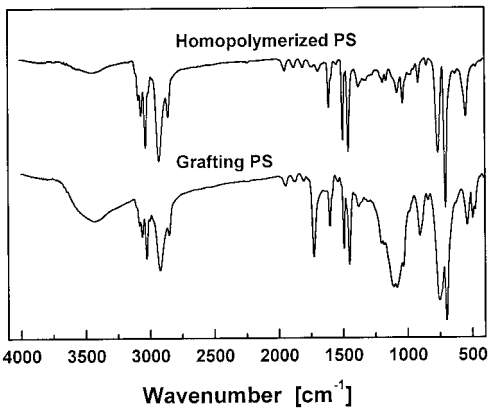

Figure 6 FTIR spectra of grafting PS and homopolymerized PS.

peak pyrolysis temperature of grafting PS is 427°C, which is significantly lower than that of SiO_2-*g*-PS (459°C). To examine the interaction between KH570 silica and grafting PS from another angle, we used XPS to characterize the surface group interaction. Figure 8 compares the C1s spectrum of neat PS with SiO_2-*g*-PS and the O1s spectrum of KH570-treated SiO_2 with SiO_2-*g*-PS. It is evident that the carbon atoms become electron-rich because the C1s peak of aromatic carbon or aliphatic carbon around 284–285 eV shifts to a lower binding energy direction when PS is grafted onto the particles [Fig. 8(a)]. Furthermore, the π–π^* shake-up satellite peak in the spectrum of PS around 292 eV, which is associated with the presence of delocalized π electrons in a conjugated phenyl system, completely disappear in SiO_2-*g*-PS. As the intensity of this peak can be greatly reduced with an electron transfer from nanoparticles to the phenyl of PS,[20] it can thus be deduced that the interaction between KH570-treated SiO_2 and PS is quite strong. Because it is not possible for electrons to transfer from oxygen atoms of KH570 to carbon atoms of PS, the aforementioned electron transfer has to proceed from silica to PS.

However, the O1s spectrum of SiO_2-*g*-PS also shows a shift to a lower binding energy direction [Fig. 8(b)], indicating that some of the carboxyl oxygen atoms become electron-rich after being grafted. This can be attributed to the formation of π complexes between KH550 and PS. The phenyl ring of PS might act as a typical nucleophilic agent. For KH570, the carboxyl oxygen atom has a strong electron-withdrawing effect on the phenylene ring and thus renders it electrophilic. As a result, the π complexes so formed cause the oxygen atom to be electron-rich.

The C1s spectra of KH570-treated SiO_2, SiO_2-*g*-PMMA, SiO_2-*g*-PEA, and SiO_2-*g*-PBA are shown in Figure 9. The peak positions or peak shapes of the C1s spectra of the grafted silica are quite different from those of the spectrum of KH570-treated SiO_2, and this suggests that the surface of silica mainly contains grafting polymers instead of KH570. As KH570 possesses an ester structure similar to that of the grafting polymers, it is difficult to analyze the interaction between the grafting polymers and KH570 only by XPS measurements. Nevertheless, as reported in ref. 21, the effect of grafted SiO_2 nanoparticles on the crystalliza-

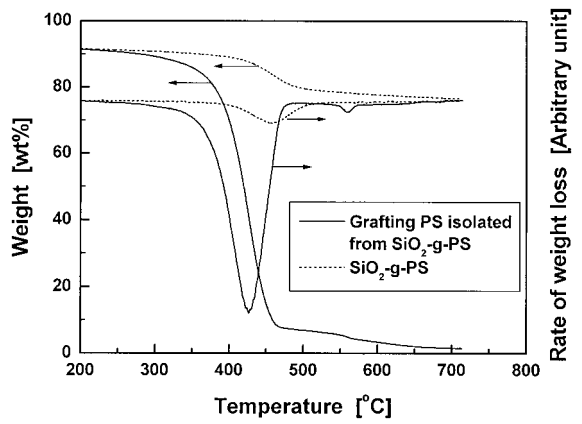

Figure 7 Thermal decomposition behaviors of grafting PS and SiO_2-*g*-PS.

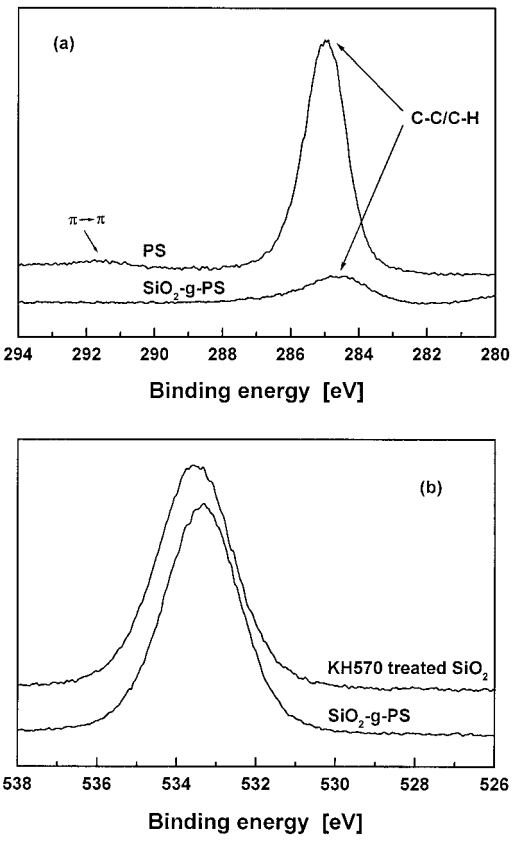

Figure 8 (a) XPS C1s spectra of PS and SiO_2-*g*-PS (γ_g = 5.6%) and (b) XPS O1s spectra of KH570-treated SiO_2 and SiO_2-*g*-PS (γ_g = 5.6%).

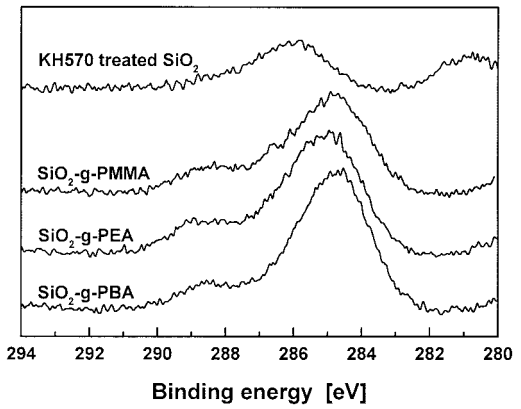

Figure 9 XPS C1s spectra of KH570-treated SiO_2, SiO_2-*g*-PMMA (γ_g = 14.1%), SiO_2-*g*-PEA (γ_g = 21.3%), and SiO_2-*g*-PBA (γ_g = 19.4%).

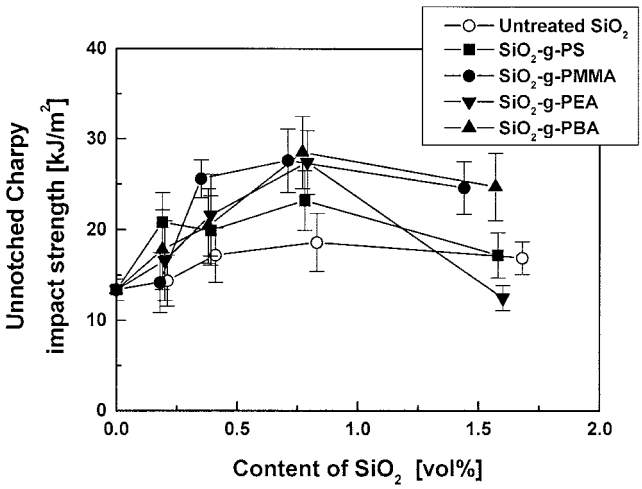

Figure 11 Unnotched Charpy impact strength of PP composites filled with untreated SiO_2, SiO_2-*g*-PS (γ_g = 5.6%), SiO_2-*g*-PMMA (γ_g = 14.1%), SiO_2-*g*-PEA (γ_g = 4.4%), and SiO_2-*g*-PBA (γ_g = 6.5%) as a function of the SiO_2 content.

tion of PP reflects the strong interaction between the nanoparticles and the grafting polymer, which increases the regularity of the grafting molecules to a certain extent.

The morphologies of the nanoparticles before and after grafting polymerization are illustrated in Figure 10. Large agglomerates of particles (~400 nm) can be observed for the silica as received, whereas the grafting treatment helps to reduce the size of the agglomerates to about 150 nm. A very thin layer of the grafting polymer covering the silica aggregates can be identified, and it should be responsible for the alteration of the interface when the particles are used to reinforce PP. Meanwhile, the grafting polymer and particles build up the nanocomposite structure, which eliminates the loose structure of the agglomerated nanoparticles and should be beneficial to the mechanical performance of silica/PP composites.

Effect of the differently grafted nanoparticles on the impact resistance of PP composites

Intuitively, it is believed that the features of the filler–matrix interfacial layer are responsible to a great extent for the impact properties of PP composites. When ungrafted nano-silica is added to PP, a mild increase in the impact strength is measured up to 0.8 vol % (Fig. 11). Above this filler content, there is a decreasing trend in the impact strength with an increasing content of silica. It can be attributed to the worse dispersion of nanoparticles in the PP matrix at higher filler contents. The loosened clusters of the nanoparticles are surely detrimental to the impact toughness of the composites.

The effects of different grafted nano-silicas on the impact strength of PP composites are plotted as a

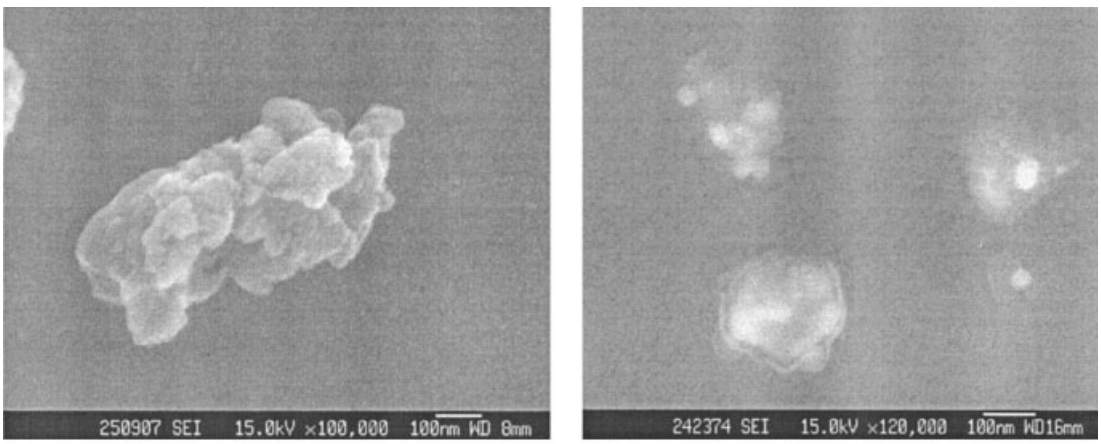

Figure 10 Scanning electron microscopy images of (a) untreated SiO_2 and (b) SiO_2-*g*-PMMA (γ_g = 14.1%).

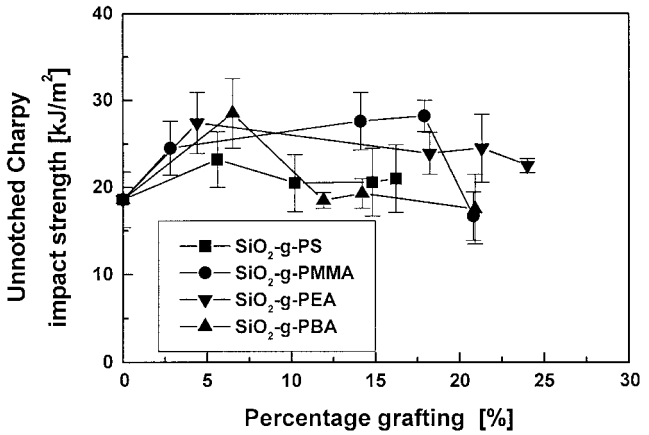

Figure 12 Unnotched Charpy impact strength of PP composites filled with SiO_2-*g*-PS, SiO_2-*g*-PMMA, SiO_2-*g*-PEA, and SiO_2-*g*-PBA as a function of γ_g at a constant filler loading of 0.8 vol %.

function of the filler content in Figure 11. The grafting polymers, which encapsulate silica particles, result in an evident increase in the impact strength in comparison with the untreated silica counterpart. This means that an interphase consisting of the grafting polymers, especially those with higher molecular mobility such as PEA and PBA, might act as a bumper interlayer around the fillers. It absorbs the impact energy and prevents the initiation of cracks. Besides, the nanoparticle–matrix adhesion created by the entangled interphase between the grafting polymer and the matrix can also obstruct crack propagation at the interface. There exists an optimum value for the dependence of the impact strength on the filler content (~0.8 vol %). This can still be explained by the poorer dispersion of the particles at higher filler contents, being similar to the case of untreated silica-filled PP.

The previous discussion is focused mainly on the effects of the species of the grafting polymer and the contents of grafted nano-SiO_2 on the impact strength of nano-silica-filled PP. In fact, the structure and viscoelastic characteristics of the interphase also play important roles. At a constant filler loading, the influence of the amount of the grafting polymers on nano-SiO_2 is shown in Figure 12. A high value of γ_g is generally disadvantageous to the improvement of the impact strength for the nanocomposites. If the interphase thickness can be assumed to increase with the grafting polymer fraction, the impact strength should increase because of the possible increase in the interface entanglement. However, that is not the case. Therefore, the evident toughening effect perceived at such low γ_g values in these nanocomposites implies that other factors should account for the mechanism involved besides interfacial adhesion, which restricts the propagation of cracks. Hasegawa et al.[22] investigated the distribution of polymer-grafted particles in a polymer matrix and found that there was an optimum grafting density for the good dispersion of the particles. Tada et al.[23] also pointed out the importance of the optimum molecular weight of the grafting polymer in the dispersibility of TiO_2 particles. It can be imagined that the severe entanglement of grafting polymers at high γ_g values might hinder the separation of nanoparticle agglomerates in the matrix polymer. Consequently, the greatest contribution of grafted SiO_2 nanoparticles to the improvement of the impact properties of PP composites is observed at low γ_g values. For the moment, the optimum γ_g value that facilitates nanoparticle dispersion for the current composites is hard to determine on the basis of the impact performance data because most composites filled with grafted nanoparticles having different γ_g values possess an impact strength higher than that of untreated nano-SiO_2/PP composites (Fig. 12). Much more work is needed for a deeper understanding.

Effect of differently grafted nanoparticles on the tensile properties of PP composites

It is well known that Young's modulus of particulate composites is highly related to the filler–matrix interfacial interaction.[24] As it is measured within a small strain region, the static stress transfer efficiency at the interface can be revealed. The stiffness measurements of these composites show that at low filler contents (<0.8 vol %), the grafted nano-silica particles provide PP with a higher modulus than the untreated ones in most cases (Fig. 13). When the filler content is increased (e.g., 1.6 vol %), however, the grafting layer tends to hinder complete stress transfer, especially for PEA- and PBA-grafted silica, leading to lower stiffness of the composites. Because γ_g of the nanoparticles is constant for each group of composites, the interfacial

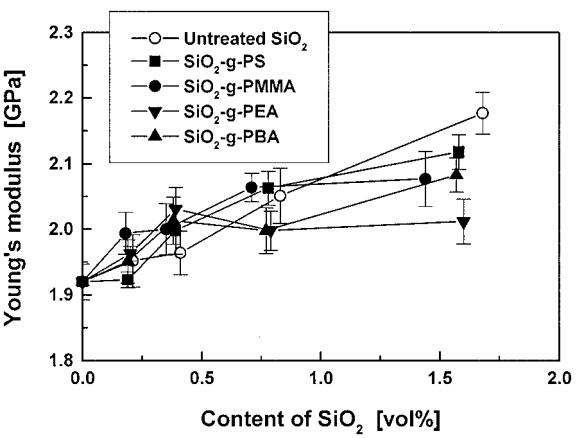

Figure 13 Young's modulus of PP composites filled with untreated SiO_2, SiO_2-*g*-PS (γ_g = 5.6%), SiO_2-*g*-PMMA (γ_g = 14.1%), SiO_2-*g*-PEA (γ_g = 4.4%), and SiO_2-*g*-PBA (γ_g = 6.5%) as a function of the SiO_2 content.

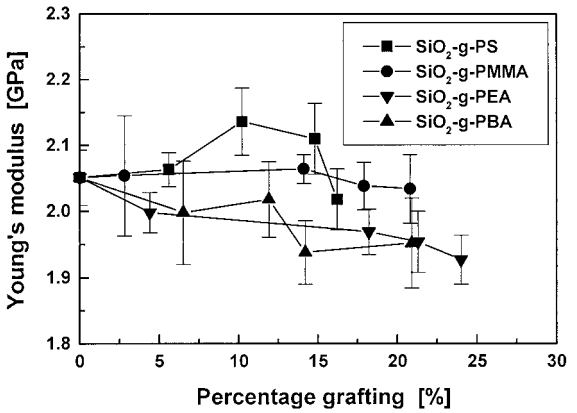

Figure 14 Young's modulus of PP composites filled with SiO_2-*g*-PS, SiO_2-*g*-PMMA, SiO_2-*g*-PEA, and SiO_2-*g*-PBA as a function of γ_g at a constant filler loading of 0.8 vol %.

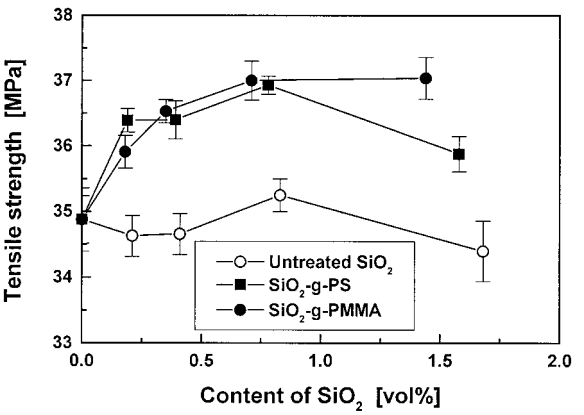

Figure 15 Tensile strength of PP composites filled with untreated SiO_2, SiO_2-*g*-PS (γ_g = 5.6%), and SiO_2-*g*-PMMA (γ_g = 14.1%) as a function of the SiO_2 content.

adhesion should not change with the filler content. Consequently, the decrease in the modulus might again be related to the dispersion of the fillers in the matrix polymer. The loose structure of silica agglomerates at higher filler loading is undoubtedly detrimental to stress transfer, even under the conditions for which Hooke's law is valid. In addition, the compliant nature of PEA and PBA molecules also result in a lower modulus of the composites, as demonstrated by a comparison of the data of SiO_2-*g*-PEA and SiO_2-*g*-PBA with those of SiO_2-*g*-PS with similar γ_g values of the nanoparticles (Fig. 13).

Demjen and Pukanszky[25] reported that for a coupling agent treatment, the particulate composite stiffness usually decreases somewhat as the coupling agent concentration increases. The explanation for this phenomenon is the formation of a multilayer interface of inferior properties, which allows dewetting even at low deformation. Through an examination of the effect of γ_g on Young's modulus of these composites at a constant SiO_2 content (Fig. 14), we have found that the situation is not the same as that for the silane coupling treatment previously mentioned. Different species of the grafting polymer cause different results. For SiO_2-*g*-PS/PP composites, the modulus increases first and then decreases with a rise in γ_g of the nanoparticles. In the case of SiO_2-*g*-PMMA/PP composites, the modulus is nearly unchanged within the testing range of γ_g of the nanoparticles, whereas SiO_2-*g*-PEA/PP and SiO_2-*g*-PBA/PP composites always exhibit a declining trend. It is evident that the features of the grafting polymers and their diffusion into the matrix are responsible for the different responses. PS molecular chains are stiffer than those of PMMA, PEA, and PBA, and this accounts for the fact that the composites filled with SiO_2-*g*-PS have a higher modulus and that those with SiO_2-*g*-PBA have the lowest modulus. Even though no difference is evident between the solubility parameters of PP [16.7–18.8 $(J/mol)^{1/2}$], PS [17.4–19.0 $(J/mol)^{1/2}$], PMMA [18.6–22.4 $(J/mol)^{1/2}$], PEA [19.2 $(J/mol)^{1/2}$], and PBA [18.0–18.6 $(J/mol)^{1/2}$], the molecules of PMMA might be more flexible than those of PS, and this could lead to a specific stiffening behavior of the treated nanoparticles different from that of SiO_2-*g*-PS, SiO_2-*g*-PEA, or SiO_2-*g*-PBA.

In Figures 15 and 16, the effects of PS, PMMA, PEA, and PBA grafting onto nano-SiO_2 on the tensile strength of the composites are compared with the effects of untreated nano-silica. Obviously, the incorporation of untreated nano-SiO_2 tends to lower the tensile strength of PP in most cases. In contrast, the improvement of interfacial adhesion due to the introduction of the grafting polymers to the nanoparticles is able to strengthen PP. That is, in the composites filled with grafted nano-SiO_2, the applied load seems to be effectively transferred from the matrix to the filler particles because of the adhesive effect of the grafting polymers by interfacial entanglement with PP molecules. A careful survey of the plots given in Fig-

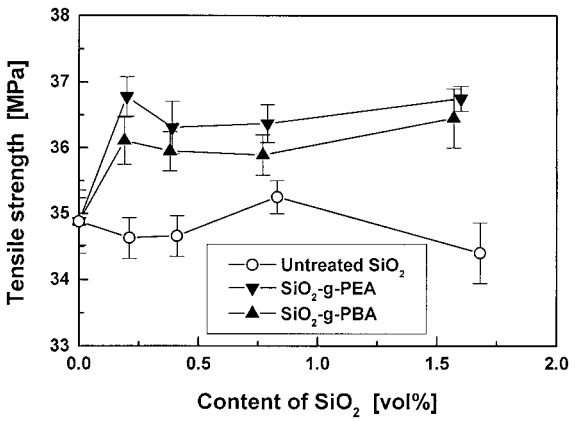

Figure 16 Tensile strength of PP composites filled with untreated SiO_2, SiO_2-*g*-PEA (γ_g = 4.4%), and SiO_2-*g*-PBA (γ_g = 6.5%) as a function of the SiO_2 content.

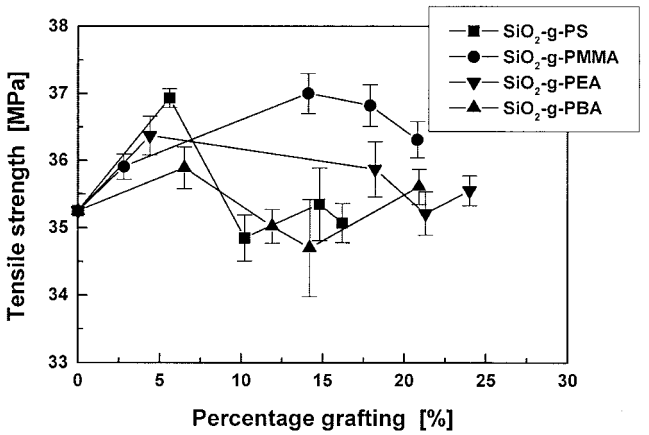

Figure 17 Tensile strength of PP composites filled with SiO_2-*g*-PS, SiO_2-*g*-PMMA, SiO_2-*g*-PEA, and SiO_2-*g*-PBA as a function of γ_g at a constant filler loading of 0.8 vol %.

ures 15 and 16 indicates that the filler content dependences of the tensile strength of the composites with different grafted nanoparticles are different, except for a drastic increase at a rather low filler loading (~0.2 vol %). It factually reflects the role of the interfacial effect. With respect to PS- and PMMA-grafted nano-SiO_2-filled PP composites (Fig. 15), the strength moderately increases up to 0.8 vol %. When the SiO_2 content is raised further, the strength of SiO_2-*g*-PS/PP decreases, probably because of a worse dispersion of the nanoparticles, but that of SiO_2-*g*-PMMA/PP does not vary; this implies that higher miscibility between PMMA and PP helps to establish stronger interfacial bonding between the nanoparticles and PP matrix.

In the case of PEA- and PBA-grafted SiO_2-filled PP composites (Fig. 16), there is an increasing trend in the tensile strength at a higher filler loading (~1.6 vol %). It represents competition between the effects of the interface adhesion and filler concentration. As discussed previously, the interphase formed in PEA- and PBA-grafted nano-SiO_2/PP composites is softer than that in PS- and PMMA-grafted nano-SiO_2/PP composites. The lowest strengthening efficiency of the composites with SiO_2-*g*-PBA supports the idea that stress transfer at this kind of interphase is less effective. Nevertheless, the soft interlayer might be able to hinder the development of cavities, which merge rapidly to crack. With respect to this, the negative effect generated by a soft interface might be compensated by the positive effect (i.e., increased resistance to cavitation) at a higher filler loading. However, at a low filler concentration (e.g., 0.8 vol %), an increase in the interphase thickness is certainly detrimental to the strengthening of the composites because of the masking effect on stress transfer (Fig. 17). Similarly, the systems with PMMA-grafted nano-silica possess a stable strengthening effect over the testing range of γ_g of the nanoparticles, and this indicates the better solubility of grafting PMMA with the PP matrix.

Although the values of the elongation to break measured in this work are associated with considerable deviations (as characterized by the large error bars in Fig. 18), the preliminary results show that the toughening effect of the polymer-grafted nanoparticles on PP composites is superior to that of untreated nanosilica. Especially when the filler content is around 0.8 vol %, the values of the elongation to break of SiO_2-*g*-PS/PP and SiO_2-*g*-PMMA/PP composites reach the maxima (Fig. 18), whereas their tensile strengths remain on a high level (Fig. 15). The reinforcing effects of the grafting polymers chemically attached to the nanoparticles on both the strength and elongation to break of PP composites must stem from their high-molecular-weight feature and entanglement with matrix polymers. Unlike the multilayer established by a silane coupling agent on a particulate filler surface,[25] the interfacial layer in these nanocomposites is difficult to remove and leads to a stronger interfacial interaction. Moreover, the deformation of this interphase might also increase the elongation to break of the composites. A detailed study of the effect of interfacial tailoring on the elongation to break of PP nanocomposites will be carried out on injection-molding specimens soon.

CONCLUSIONS

Grafting polymerization onto nanoparticles provides polymeric composites with tailorable interphases. On the basis of the results of PP/silica composites, we know that filler–matrix interfacial adhesion can be improved by the grafting polymers chemically bonded onto the nanoparticles, which create entanglements with the matrix molecules. The characteristics

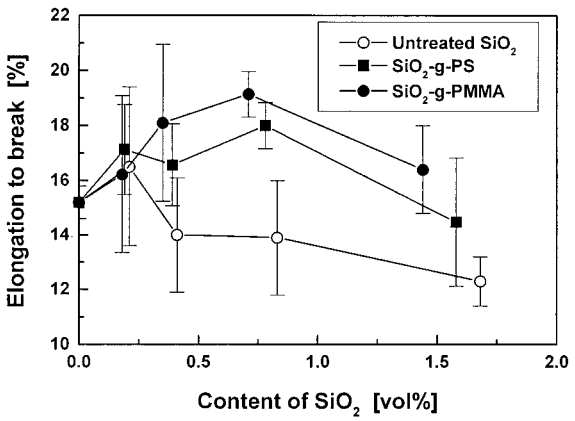

Figure 18 Elongation to break of PP composites filled with untreated SiO_2, SiO_2-*g*-PS (γ_g = 5.6%), and SiO_2-*g*-PMMA (γ_g = 14.1%) as a function of the SiO_2 content.

of grafting polymers on nano-silica, including molecular stiffness, molecular solubility with the matrix, and grafting density, exert great influence on the reinforcement effectiveness of PP composites. The grafting polymer, especially one with higher molecular mobility such as PEA and PBA, increases the impact strength in comparison with the untreated silica counterpart. The mechanism can be ascribed to the energy absorption and hindering effect on crack propagation by the interphase. To make the most of the modified nanoparticles, it is preferable to control the γ_g values of the fillers at a low level to achieve better dispersion of the particles in the PP matrix. The tensile performance of the composites is also highly dependent on the nature of the grafting polymers on the nanoparticles. The stiff interphase created by PS- and PMMA-grafted nano-SiO_2 is beneficial to the enhancement of the modulus and strength of the composites, whereas the relatively soft interphases in SiO_2-*g*-PEA/PP and SiO_2-*g*-PBA/PP composites are more suitable for use at higher SiO_2 loadings to obstruct the development of cavities. To simultaneously increase both Young's modulus and the tensile strength of PP composites, we suggest a thin interlayer because the filler dispersion can be improved.

The results and discussions given in this article show the necessity of modeling that considers both the interfacial features and filler concentration in modified nanoparticle/polymer composites. It is also important to take γ_g and the solubility of the grafting polymer with the matrix into account. This remains to be studied in the future as one part of our series on polymer nanocomposites.

The authors are grateful for the cooperation between the German and Chinese institutes on the topic of nanocomposites.

References

1. Kurokawa, Y.; Yasudo, H.; Kashiwagi, M.; Oyo, A. J Mater Sci Lett 1997, 16, 1670.
2. Yano, K.; Yuranchi, T.; Kamigaito, O. J Appl Polym Sci 1993, 31, 2493.
3. Kawasumi, M.; Hasegawa, N.; Kato, M.; Usuki, A.; Okada, A. Macromolecules 1997, 30, 6333.
4. Chen, Y.; Iroh, J. O. Chem Mater 1999, 11, 1218.
5. Usuki, A.; Kojima, Y.; Kawasumi, M.; Okada, A.; Fukushima, Y.; Kuroachi, T.; Kaimigato, O. J Mater Res 1993, 8, 1179.
6. Wang, M. S.; Pinnavaia, T. J. Chem Mater 1994, 6, 468.
7. Yang, F.; Ou, Y.; Yu, Z. J Appl Polym Sci 1998, 69, 355.
8. Pozsgay, A.; Frater, T.; Papp, L.; Sajo, I.; Pukanszky, B. J Macromol Sci Phys 2002, 41, 1249.
9. Gopakumar, T. G.; Lee, J. A.; Kontopoulou, M.; Parent, J. S. Polymer 2002, 43, 5483.
10. Sun, T.; Garces, J. M. Adv Mater 2002, 14, 128.
11. Chan, C. M.; Wu, J. S.; Li, J. X.; Cheung, Y. K. Polymer 2002, 43, 2981.
12. Wang, G.; Chen, X. Y.; Huang, R.; Zhang, L. J Mater Sci Lett 2002, 21, 985.
13. Saujanya, C.; Radhakrishnan, S. Polymer 2001, 42, 6723.
14. Rong, M. Z.; Zhang, M. Q.; Zheng, Y. X.; Zeng, H. M.; Walter, R.; Friedrich, K. J Mater Sci Lett 2000, 19, 1159.
15. Rong, M. Z.; Zhang, M. Q.; Zheng, Y. X.; Zeng, H. M.; Walter, R.; Friedrich, K. Polymer 2001, 42, 167.
16. Zhang, M. Q.; Rong, M. Z.; Zeng, H. M.; Schmitt, S.; Wetze, B.; Friedrich, K. J Appl Polym Sci 2001, 80, 2218.
17. Wu, C. L.; Zhang, M. Q.; Rong, M. Z.; Friedrich, K. Compos Sci Technol 2002, 62, 1327.
18. Zhang, M. Q.; Rong, M. Z.; Pan, S. L.; Friedrich, K. Adv Compos Lett 2002, 11, 291.
19. Rong, M. Z.; Zhang, M. Q.; Zheng, Y. X.; Zeng, H. M.; Friedrich, K. Polymer 2001, 42, 3301.
20. Zeng, R.; Rong, M. Z.; Zhang, M. Q.; Liang, H. C.; Zeng, H. M. J Mater Sci Lett 2001, 20, 1473.
21. Pan, S. L. Master Thesis, Zhongshan University, 2002 (in Chinese).
22. Hasegawa, R.; Aoki, Y.; Doi, M. Macromolecules 1996, 29, 6656.
23. Tada, H.; Saito, Y.; Hyodo, M. J Colloid Interface Sci 1993, 159, 249.
24. Pukanszky, B.; Fekete, E.; Tudos, F. Macromol Chem Macromol Symp 1989, 28, 165.
25. Demjen, Z.; Pukanszky, B. Polym Compos 1997, 18, 741.